NASA/CR—2007-215012

Development of a Linear Stirling System Model With Varying Heat Inputs

Timothy F. Regan and Edward J. Lewandowski
Sest, Inc., Middleburg Heights, Ohio

December 2007

NASA STI Program . . . in Profile

Since its founding, NASA has been dedicated to the advancement of aeronautics and space science. The NASA Scientific and Technical Information (STI) program plays a key part in helping NASA maintain this important role.

The NASA STI Program operates under the auspices of the Agency Chief Information Officer. It collects, organizes, provides for archiving, and disseminates NASA's STI. The NASA STI program provides access to the NASA Aeronautics and Space Database and its public interface, the NASA Technical Reports Server, thus providing one of the largest collections of aeronautical and space science STI in the world. Results are published in both non-NASA channels and by NASA in the NASA STI Report Series, which includes the following report types:

- TECHNICAL PUBLICATION. Reports of completed research or a major significant phase of research that present the results of NASA programs and include extensive data or theoretical analysis. Includes compilations of significant scientific and technical data and information deemed to be of continuing reference value. NASA counterpart of peer-reviewed formal professional papers but has less stringent limitations on manuscript length and extent of graphic presentations.

- TECHNICAL MEMORANDUM. Scientific and technical findings that are preliminary or of specialized interest, e.g., quick release reports, working papers, and bibliographies that contain minimal annotation. Does not contain extensive analysis.

- CONTRACTOR REPORT. Scientific and technical findings by NASA-sponsored contractors and grantees.

- CONFERENCE PUBLICATION. Collected papers from scientific and technical conferences, symposia, seminars, or other meetings sponsored or cosponsored by NASA.

- SPECIAL PUBLICATION. Scientific, technical, or historical information from NASA programs, projects, and missions, often concerned with subjects having substantial public interest.

- TECHNICAL TRANSLATION. English-language translations of foreign scientific and technical material pertinent to NASA's mission.

Specialized services also include creating custom thesauri, building customized databases, organizing and publishing research results.

For more information about the NASA STI program, see the following:

- Access the NASA STI program home page at *http://www.sti.nasa.gov*

- E-mail your question via the Internet to *help@sti.nasa.gov*

- Fax your question to the NASA STI Help Desk at 301–621–0134

- Telephone the NASA STI Help Desk at 301–621–0390

- Write to:
  NASA Center for AeroSpace Information (CASI)
  7115 Standard Drive
  Hanover, MD 21076–1320

NASA/CR—2007-215012

Development of a Linear Stirling System Model With Varying Heat Inputs

Timothy F. Regan and Edward J. Lewandowski
Sest, Inc., Middleburg Heights, Ohio

Prepared for the
Fifth International Energy Conversion Engineering Conference and Exhibit (IECEC)
sponsored by the American Institute of Aeronautics and Astronautics
St. Louis, Missouri, June 25–27, 2007

Prepared under Contract NNC07TA38T

National Aeronautics and
Space Administration

Glenn Research Center
Cleveland, Ohio 44135

December 2007

Acknowledgments

This work was performed for NASA Headquarters, Science Mission Directorate under the Radioisotope Power Systems program and was supported by the NASA Glenn Research Center.

Level of Review: This material has been technically reviewed by expert reviewer(s).

Available from

NASA Center for Aerospace Information
7115 Standard Drive
Hanover, MD 21076–1320

National Technical Information Service
5285 Port Royal Road
Springfield, VA 22161

Available electronically at http://gltrs.grc.nasa.gov

Development of a Linear Stirling System Model With Varying Heat Inputs

Timothy F. Regan and Edward J. Lewandowski
Sest, Inc.
Middleburg Heights, Ohio 44130

Abstract

The linear model of the Stirling system developed by NASA Glenn Research Center (GRC) has been extended to include a user-specified heat input. Previously developed linear models were limited to the Stirling convertor and electrical load. They represented the thermodynamic cycle with pressure factors that remained constant. The numerical values of the pressure factors were generated by linearizing GRC's nonlinear System Dynamic Model (SDM) of the convertor at a chosen operating point. The pressure factors were fixed for that operating point, thus, the model lost accuracy if a transition to a different operating point were simulated. Although the previous linear model was used in developing controllers that manipulated current, voltage, and piston position, it could not be used in the development of control algorithms that regulated hot-end temperature. This basic model was extended to include the thermal dynamics associated with a hot-end temperature that varies over time in response to external changes as well as to changes in the Stirling cycle. The linear model described herein includes not only dynamics of the piston, displacer, gas, and electrical circuit, but also the transient effects of the heater head thermal inertia. The linear version algebraically couples two separate linear dynamic models, one model of the Stirling convertor and one model of the thermal system, through the pressure factors. The thermal system model includes heat flow of heat transfer fluid, insulation loss, and temperature drops from the heat source to the Stirling convertor expansion space. The linear model was compared to a nonlinear model, and performance was very similar. The resulting linear model can be implemented in a variety of computing environments, and is suitable for analysis with classical and state space controls analysis techniques.

Nomenclature

A_d	Displacer area (m^2)
A_p	Piston area (m^2)
A_{rod}	Displacer rod area (m^2)
C_h	Heater head thermal capacitance (J/K)
C_t	Tuning capacitance (μF)
D_d	Displacer damping (N-s/m)
D_p	Piston damping (N-s/m)
f	Operating frequency (Hz)
I_{alt}	Alternator current (A)
K_{bounce}	Bounce space spring rate (N/m)
K_d	Displacer spring rate (N/m)
K_{magnet}	Alternator magnet space spring rate (N/m)
K_p	Piston spring rate (N/m)
L_{alt}	Alternator inductance (H)
M_d	Effective displacer mass (kg)
M_p	Effective piston mass (kg)
MW	Gas molecular weight
N	Number of turns on the alternator winding
P	Stirling cycle dynamic pressure (Pa)
P_c	Compression space pressure (Pa)
P_d	Displacer pressure factor (Pa/m)
P_e	Expansion space pressure (Pa)
P_{exp}	Expansion space PV power (W)
P_p	Piston pressure factor (Pa/m)
Q_e	Heat into the Stirling cycle (W)
Q_{in}	Heat delivered by the heat source (W)
Q_{out}	Heat rejected (W)
R_{alt}	Alternator resistance (Ω)
R_c	Compression space resistance (W/m-K)
R_e	Expansion space resistance (W/m-K)
R_{gas}	Gas constant (J/kg-K)
R_h	Heater head resistance (W/m-K)
R_{hh}	Heater head conduction loss resistance (W/m-K)
R_{ins}	Insulation resistance (W/m-K)
t	time (sec)
T_a	Ambient temperature (K)
T_{alt}	Alternator temperature (K)
T_c	Compression space temperature (K)
T_e	Expansion space temperature (K)
T_h	Hot heat exchanger temperature (K)
T_k	Cold heat exchanger temperature (K)
T_r	Regenerator space temperature (K)
T_{source}	Heat source temperature (K)
V_c	Compression space volume (m^3)
V_{co}	Mean compression space volume (m^3)
V_e	Expansion space volume (m^3)
V_{eo}	Mean expansion space volume (m^3)
V_h	Hot heat exchanger volume (m^3)
V_k	Cold heat exchanger volume (m^3)

V_r	Regenerator volume (m^3)	η_{mag}	Alternator magnetic efficiency
x_d	Displacer position (m)	Φ	Flux (Wb)
X_d	Displacer position amplitude (m)	Φ_d	Displacer phase angle (deg)
x_p	Piston position (m)	Φ_p	Pressure phase angle (deg)
X_p	Piston position amplitude (m)	ω	Operating frequency (rad/sec)
ΔP	Pressure drop across regenerator, heater and cooler (Pa)		

I. Introduction

NASA's Glenn Research Center is using its System Dynamic Model (SDM) to develop linear models of free-piston Stirling convertors for use in real-time simulations of Stirling convertors. The outputs of such a simulation could be used in place of actual convertor hardware in tests of controllers and other convertor support hardware. The SDM is a non-linear model that simulates Stirling convertor system dynamics for systems of arbitrary complexity. SDM has been used to simulate a dual-convertor system with controllers based on pulse-width modulated (pwm) power electronics, however the maximum time step allowed for a 50 kHz pwm controller simulation is on the order of nano-seconds. Consequently, no more than a few cycles of such a system can be simulated on SDM running on a typical desk-top computer. On the other end of the spectrum, when the slow variation of system temperatures requires study, the simulation times can become so long as to make the simulation approach impractical. To address these extremes, SDM was used to linearize the model at an operating point and the linearized coefficients were used to build a linear model. Linear models run faster than SDM and they can run in a variety of computing hardware environments. Linear models of Stirling convertor systems, including a dual-opposed system and a single convertor system with a balancer were analyzed in detail as part of NASA GRC's Stirling convertor modeling effort[1]. The models reported in the literature have included only the mechanical and mounting dynamics. The pressure wave was modeled by constants—called pressure factors—that were calculated by SDM to represent the pressure wave at the point at which the model was linearized. The models described in Ref. 1 were not equipped to track the relationship between output power, hot-end temperature and piston amplitude. Convertor conditions which cause an increase or decrease of hot-end temperature such as a change in piston amplitude, a change in the input heat or the rejection temperature were not tracked successfully by those linear models. The models lost some accuracy whenever the operating point moved away from the operating point at which the model was linearized. That is, the more the piston amplitude, hot-end temperature or output power changed during a simulation using the models described in Ref. 1, the less accurate the results became. Such a model was not useful in controlling against disturbances in thermal environment or user load since disturbances in these areas invalidate the model.

The linear models developed so far have followed the state-variable formulation in which the system matrix—the A-matrix—was constrained to have constant coefficients. If the system changes with operating conditions, then the coefficients in the model cannot remain constant. In the present work, a method is described for re-computing the hot-end temperature based on the calculated expansion space PV power and re-computing certain entries in the A-matrix as the system temperatures change.

The validation data for the models described herein were published by NASA in 1999 from operation of the Component Test Power Convertor (CTPC). The CTPC effort published design details as well as test data. The final report[2,3] has been used for validation of Stirling simulation codes and design codes. A model of the CTPC was constructed in SDM and used to produce linearized A-matrix coefficients as in the models described in Ref. 1. Section II begins with a description of the CTPC and its SDM model. Section II-A describes the linear electro-mechanical model. Section II-B describes the thermal system model. Section II-C describes how the models are coupled through re-computation of the pressure factors. Section III summarizes the results.

II. CTPC Dynamic Model

A high-level schematic of the SDM model of the CTPC is shown in figure 1. Starting at the bottom of the figure, the heat input to the Stirling cycle was represented by the heat input Q_{in}, shown with two flow paths emanating from it. One flow path represents the heat lost through the insulation to ambient and has the thermal resistance R_{ins}. The other flow path represents the heat conducted to the heater. There is a temperature drop from the heat source to the heater. The temperature drop was modeled by the resistance R_h. The thermal time constant of the heat input system was modeled by the thermal capacitance C_h. This parameter was determined based on the mass of the CTPC heater and its heat capacity.

Not all of the heat entering the heater in the Stirling convertor goes into the Stirling cycle. Some is conducted to the cold end through paths including the heater head wall, inner cylinder, helium gas, regenerator matrix and the displacer. This loss was modeled by the heat flow through the thermal resistance R_{hh}.

The Stirling cycle thermodynamics were modeled based on the Schmidt model[4], which assumes an isothermal Stirling cycle, but in which pumping losses through heat exchangers and the regenerator were considered. The thermodynamic portion of the model determines the internal expansion space and compression space gas pressures P_e and P_c. These pressures generate the driving forces on the displacer mass M_d and the piston mass M_p. In the model, gas spring and damping forces on the displacer were represented by K_d and D_d. Displacer damping is a non-linear function of fluid flow through the porous regenerator material and through the heat exchanger tubes. The piston is subjected to conservative forces from the bounce space gas spring and the magnet spring. In the model, these were represented by K_{bounce} and K_{magnet}. The electrical load circuit also contributes spring force if the reactance of the alternator winding is not completely balanced by the capacitive reactance of the tuning capacitor. .

The alternator produces a damping force on the piston based on the alternator current. Alternator electrical dynamics were determined by the alternator resistance, inductance, motor constant, and the tuning capacitor.

The Stirling convertor was assumed to be rigidly connected to the ground. Casing motion, dual-opposed dynamics, and the effect of a dynamic balancer could be added to this model if desired.

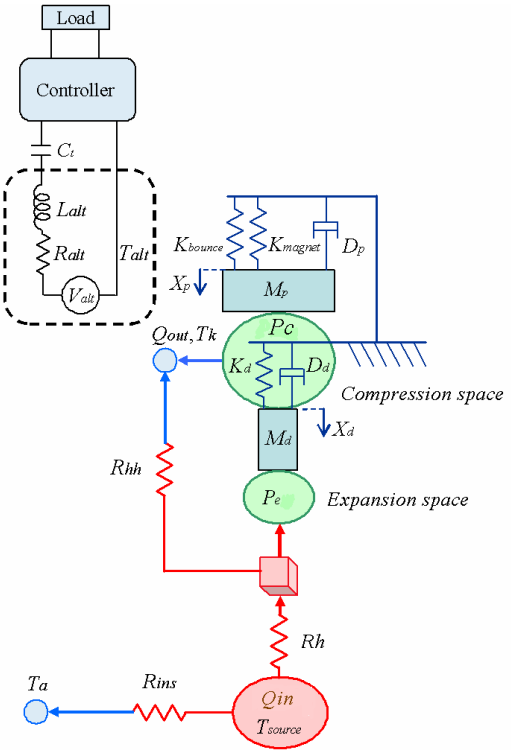

Figure 1.—Schematic of the CTPC dynamic model.

A. Linear Dynamic Stirling Model

The ultimate design of a model is determined by a number of factors, including fidelity required, simulation time, and model platform. Linearized parameters were used to create a model in Simplorer (Ansoft Corporation) and other dynamic modeling platforms. The equations for the electro-mechanical portion of the model were developed in Reference 1 and are reprinted as eqs. (1) through (4) below:.

$$\frac{dx_d}{dt} = \dot{x}_d \tag{1}$$

$$\frac{d\dot{x}_d}{dt} = -\left(K_d + A_r \frac{\partial P}{\partial x_d}\right)\frac{1}{M_d}x_d + \left(A_d \frac{\partial \Delta P}{\partial \dot{x}_d}\right)\frac{1}{M_d}\dot{x}_d - A_r \frac{\partial P}{\partial x_p}\frac{1}{M_d}x_p + \left(A_d \frac{\partial \Delta P}{\partial \dot{x}_p}\right)\frac{1}{M_d}\dot{x}_p \tag{2}$$

$$\frac{dx_p}{dt} = \dot{x}_p \tag{3}$$

$$\frac{d\dot{x}_p}{dt} = -A_p \frac{\partial P}{\partial x_d}\frac{1}{M_p}x_d - \left(K_p + A_p \frac{\partial P}{\partial x_p}\right)\frac{1}{M_p}x_p - \frac{D_p}{M_p}\dot{x}_p + N\frac{d\Phi}{dx_p}\frac{1}{\eta_{mag}}\frac{1}{M_p}I_{alt} \tag{4}$$

Equations (1) through (4) represent the dynamic equations for the displacer and the piston. In eq. (2), the force due to the pressure wave's action on the displacer area A_d has been accounted for in two parts. This is because the pressure is expressed as a linear combination of the piston and displacer positions. To reconstruct the pressure wave,

the contribution of both components must be considered. The same discussion applies to the pressure force on the piston in eq. (4). In state-variable format,

$$\dot{X} = A \cdot X + B \cdot u \tag{5a}$$

with the state vector defined as

$$X = \begin{bmatrix} x_d & \dot{x}_d & x_p & \dot{x}_p \end{bmatrix}^T , \tag{5}$$

the ***A***-matrix entries are seen to be the coefficients of the state variables in eqs. (1) through (4), above. In eq. (4), the right-most term expresses the piston damping due to alternator current. In a state-variable formulation, I_{alt} is the input, u, and the coefficient of I_{alt} is the ***B***-matrix entry that contributes to eq. (4). Thus,

$$B = \begin{bmatrix} 0 & 0 & 0 & N\dfrac{d\Phi}{dx_p}\dfrac{1}{\eta_{mag}}\dfrac{1}{M_p} \end{bmatrix}^T . \tag{6}$$

B. Thermal System Model

Figure 2 shows the thermal system modeled as a series of thermal resistances with a heat capacitance, heat input, and temperature sinks. It is analogous to figure 1 with the electromechanical components removed. The schematic shows the system as it is configured in the Simplorer modeling platform

Thermal energy from the heater Q_{in} is shown to be divided between two flow paths: 1) heat lost through the insulation to ambient was determined from R_{ins} and 2) heat transferred to the heater head was determined from R_h. The resulting heat flow to the heater head causes an increased convertor hot-end temperature T_h.

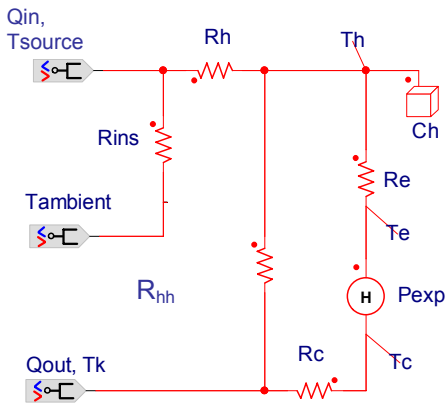

Figure 2.—The thermal system was modeled as a circuit in SDM.

Thermal energy from T_h is shown to be divided among three flow paths: 1) heat lost via conduction through the convertor was determined from R_{hh}, 2) heat transferred to the gas in the expansion space is determined from R_e, and 3) heat transferred to the heater head material was determined from the heater head thermal capacitance C_h. Thermal capacitance only becomes apparent during transient analysis; at steady-state operation the heater head material temperature equals T_h, and heat flow is divided between the conduction loss and heating of the gas expansion space, with the bulk of the heat being transferred to the latter.

Heat is rejected from the convertor to the cold-sink temperature T_k. Most of the rejected heat flows from the working fluid. The remainder of the heat rejected is from the conduction losses. The circuit model shown in figure 2 displays the operation of the thermal system. Circuit solvers such as the one included with Simplorer offer a convenient way to calculate the temperatures and heat flows throughout the thermal system. Simplorer will not simulate the solution in real time however. To implement a Stirling convertor simulator in real time, the circuit solution must be implemented in more direct mathematical language. The method presented here follows a state variable formulation. There is one energy storage element in the thermal system: the heater head thermal mass, C_h, therefore, there is only one state variable in the formulation.

1. State Variable Formulation of the Thermal System

In the circuit diagram of figure 3, as in the circuit of figure 2, there is one energy storage element, the heater head thermal mass, C_h. The single state variable is the temperature across it, T_h. There are four inputs—the heat in, the expansion space PV power, the ambient temperature, and the rejection temperature. The inputs are Q_{in}, Q_{pv}, T_a, and T_k, respectively. Heat source Q_{in} models a fixed heat source such as a radioisotope heat source. Q_{pv} is a

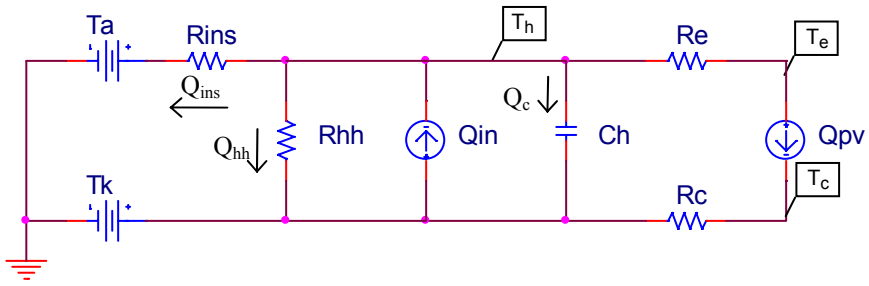

Figure 3.—A simplified circuit was used to derive the state-variable equation used in the linear model.

continuous calculation of the expansion space work over the cycle. Observe that when Q_{in} is greater than Q_{pv}, the excess heat flows into the capacitor, C_h. The temperature across C_h will rise as a result. The heat through a thermal mass (capacitance) is related to the temperature across it as shown in eq. (7).

$$Q_c = Q_{in} - Q_{pv} = C_h \frac{dT_h}{dt}. \tag{7}$$

If the heat flow into the capacitor increases, then Q_{in} will be greater than Q_{pv}, and the temperature across the capacitor will increase. If the heat flow into the capacitor decreases, then Q_{in} is less than Q_{pv}, and the temperature across the capacitor will decrease.

The circuit of figure 3 is more simple than the circuit of figure 2 in that the thermal resistor, R_h has been eliminated. This was done to simplify the math used to calculate the expansion space temperature. The process of reducing the thermal circuit of figure 3 to state-variable form was motivated by the observation that the heat supplied to the convertor by Q_{in} is the sum of the insulation loss, the heater head conduction, the expansion space PV power, and the heat into the thermal capacitance

$$Q_{in} = Q_{ins} + Q_{hh} + Q_{pv} + Q_c = Q_{ins} + Q_{hh} + Q_{pv} + C_h \frac{dT_h}{dt} \tag{8}$$

Additionally, the insulation loss and the heater head conduction can be expressed in terms of the inputs and the state variable as shown in eqs. (9) and (10).

$$Q_{ins} = \frac{T_h - T_A}{R_{ins}} \tag{9}$$

$$Q_{hh} = \frac{T_h - T_k}{R_{hh}}. \tag{10}$$

The expansion and compression space temperatures, T_e and T_c can be expressed in terms of input, Q_{pv} and the state variable, T_h, thus:

$$T_e = T_h - R_e \cdot Q_{pv} \text{ and } T_c = T_h + R_c \cdot Q_{pv} \tag{11}$$

By substituting eqs. (9) and (10) into eq. (8) and simplifying, the following expression was obtained:

$$\frac{dT_h}{dt} = \frac{-T_h(R_{hh}^{-1} + R_{ins}^{-1})}{C_h} + \frac{Q_{in}}{C_h} - \frac{Q_{PV}}{C_h} - \frac{T_k}{C_h \cdot R_{hh}} - \frac{T_A}{C_h \cdot R_{ins}} \tag{12}$$

Equation (12) is in the basic form of the state equation,

$$\dot{X} = AX + Bu \tag{13}$$

where A is the single coefficient

$$A = a_{11} = \frac{-(R_{hh}{}^{-1} + R_{ins}{}^{-1})}{C_h} \tag{14}$$

and B is the vector $[b_1\ b_2\ b_3\ b_4]^T$ where

$$b_1 = \frac{1}{C_h} \tag{15a}$$

$$b_2 = \frac{-1}{C_h} \tag{15b}$$

$$b_3 = \frac{1}{C_h \cdot R_{ins}} \tag{15c}$$

$$b_4 = \frac{1}{C_h \cdot R_{hh}} \tag{15d}$$

Thus, there is a B-vector coefficient for each of the four inputs, Q_{in}, Q_{PV}, T_A and T_k. When the product ***Bu*** is evaluated, one number is produced. It has dimensions of Kelvins per second. An implementation of the state equation in block diagram form is shown in figure 4.

The thermal model determines the hot-end temperature (T_h) for the Stirling cycle, but does not calculate cycle performance or convert heat energy into mechanical energy. This is accomplished by coupling the linear Stirling model to the thermal system model. The next section will discuss how the model coupling was performed.

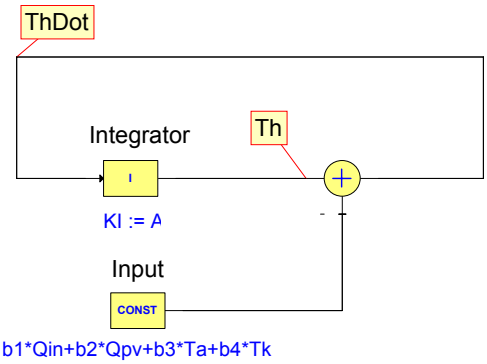

Figure 4.—Thermal model block diagram used to solve the state equation.

C. Coupling Stirling Linear Model and Thermal System Model

To complete the linear model of the CTPC, the Stirling dynamic model has to be coupled to the thermal system model. One approach would be to expand the Stirling cycle model of eqs. (1) to (4) to include the thermal system. The concern with this approach is that the response time of the Stirling cycle is on the order of milliseconds, while the response time of the thermal system are on the order of seconds or minutes. By keeping the electro-mechanical system separate from the thermal system, the likelihood of formulating an ill-conditioned matrix is reduced.

An alternative approach is to algebraically couple two separate linear dynamic models, one model of the Stirling cycle and one model of the thermal system, through the pressure factors. The pressure factors are the partial derivatives of the pressure wave P with respect to displacer position x_d and piston position x_p. The equations to couple the systems can be derived from the Stirling cycle equations as derived by Urieli and Berchowitz[4].

$$P = M_w \cdot R_{gas} \cdot \left(\frac{V_h}{T_h} + \frac{V_r}{T_r} + \frac{V_k}{T_k} + \frac{V_e}{T_e} + \frac{V_c}{T_c} \right)^{-1} \tag{16}$$

In eq. (16) the volumes V_e and V_c are functions of x_d and x_p. The other variables are assumed to be fixed over a given cycle.

$$V_e = V_{eo} - A_d x_d \tag{17}$$

$$V_c = V_{co} - A_p x_p + (A_d - A_{rod}) x_d \tag{18}$$

The temperatures T_c and T_e can be expressed in terms of the heat into the heater head Q_h based on the thermal circuit shown in figure 2, where the thermal resistance R_e is used to calculate the temperature drop from T_h to T_e, and R_c is used to calculate the temperature drop from T_c to T_k.

$$T_e = T_h - Q_h R_e \tag{19}$$

$$T_c = Q_h R_c + T_k \tag{20}$$

The regenerator temperature can be expressed as the log mean temperature between T_h and T_k:

$$T_r = \frac{T_h - T_k}{\ln(T_h / T_k)} \tag{21}$$

Substituting eqs. (17) to (20) into eq. (16) and differentiating yields the following expressions for the pressure factors

$$\frac{\partial P}{\partial x_p} = \frac{A_p M_w R_{gas}}{(Q_e R_c + T_k)} \cdot \left[\frac{V_{co} - A_p x_p + (A_d - A_{rod}) x_d}{Q_e R_c + T_k} + \frac{V_k}{T_k} + \frac{V_r \ln(T_h / T_k)}{T_h - T_k} + \frac{V_h}{T_h} + \frac{V_{eo} - A_d x_d}{T_h - Q_e R_e} \right]^{-2} \tag{22}$$

$$\frac{\partial P}{\partial x_d} = -M_w R_{gas} \left[\frac{(A_d - A_{rod})}{Q_e R_c + T_k} - \frac{A_d}{(T_h - Q_e R_e)} \right] \cdot \left[\frac{V_{co} - A_p x_p + (A_d - A_{rod}) x_d}{Q_e R_c + T_k} + \frac{V_k}{T_k} + \frac{V_r \ln(T_h / T_k)}{T_h - T_k} + \frac{V_h}{T_h} + \frac{V_{eo} - A_d x_d}{T_h - Q_e R_e} \right]^{-2} \tag{23}$$

The pressure factors are now functions of T_h, T_k, Q_e, which can be determined based on the dynamics of the thermal system. The pressure factors are also functions of x_p and x_d. In theory, the pressure factors should be the same regardless of the point in the cycle at which x_p and x_d were measured, but analysis of simulation data has shown that the calculated values of the pressure factors do vary over the cycle. It has been observed that the calculated values of the pressure factors are closest to the actual value as determined from analysis of the pressure wave when $x_p = x_d$ and are both negative. Further analysis is needed to understand the reason for this and to understand the limitations. Given displacer and piston amplitudes X_d and X_p and a displacer phase angle φ_d, x_p and x_d are equal and negative when

$$x_p = -X_p \sin\left(\tan^{-1}\left[\frac{X_d \sin\phi_d}{X_p - X_d \cos\phi_d} \right] \right) \tag{24}$$

$$x_d = -X_d \sin\left(\tan^{-1}\left[\frac{X_d \sin\phi_d}{X_p - X_d \cos\phi_d} \right] + \phi_d \right) \tag{25}$$

These values for x_p and x_d should be used in eqs. (22) and (23).

To algebraically couple the thermal system with the Stirling model, it was also necessary to calculate the expansion space PV power. The expansion space PV power is approximately equal to the heat flow into the Stirling cycle

$$\mathrm{Q}_h \approx f \oint P dV \tag{26}$$

For the expansion space,

$$V_e = V_{eo} - A_d x_d \tag{27}$$

Since

$$x_d(t) = X_d \sin(\omega t + \phi_d) \tag{28}$$

$$x_p(t) = X_p \sin(\omega t) \tag{29}$$

then

$$\frac{\mathrm{d}V_e}{dt} = -A_d X_d \omega \cos(\omega t + \phi_d) \tag{30}$$

Also, the pressure in the expansion space is a function of the pressure factors

$$P(t) = P_d x_d(t) + P_p x_p(t) \tag{31}$$

Substituting eqs. (30) and (31) into eq. (26) and integrating gives the PV power:

$$\mathrm{Q}_{pv} = \pi A_d f X_d X_p P_p \sin\phi_d \tag{32}$$

Determining the PV power is straightforward by use of eq. (32) if the phase angle and amplitudes are known. SDM makes use of Simplorer's state diagrams to calculate them from the piston and displacer position signals. The same approach can be taken with Matlab/Simulink (The MathWorks, Inc.) using the Stateflow (The MathWorks, Inc.) add-on package. Implementations that make use of the Very-high-speed integrated circuit Hardware Definition Language (VHDL) are able to use the state machine definition features of VHDL to determine amplitudes and angles. The amplitude of a sinusoidal signal can be determined by observing when the derivative of the signal crosses zero. Since the derivative of a sinusoid is a sinusoid lagging by 90°, the zero-crossing of the derivative coincides with the maximum or minimum of the original signal. Detection of zero-crossings can be detected by state machines programmed to change states when the control signal changes signs.

An even more direct solution was used in the Simplorer implementation of the linear model that did not require a state machine. The PV power was calculated by the product of frequency and the output of a power measurement block. The two inputs to the power measurement block were expansion space volume and the pressure wave instead of voltage and current.

If temperature changes in the hot end, then the working fluid redistributes itself within the working space and the non-working spaces of the convertor. The non-working spaces comprise the bounce space and the interior of the displacer. The mass of fluid in the working space is computed from the total charge, M_{tot}, as follows:

$$M_w = M_{tot} \cdot \frac{\left(\frac{V_h}{T_h} + \frac{V_r}{T_r} + \frac{V_k}{T_k} + \frac{V_{eo}}{T_e} + \frac{V_{co}}{T_c}\right)}{\left(\frac{V_h}{T_h} + \frac{V_r}{T_r} + \frac{V_k}{T_k} + \frac{V_{eo}}{T_e} + \frac{V_{co}}{T_c} + \frac{V_{bounce}}{T_{bounce}}\right)} \tag{33}$$

The pressure factors as calculated by eqs. (22) and (23) were used to re-compute the entries for a_{21}, a_{23}, and a_{41} in eqs. (34) through (36).

$$a_{21} = -\left(K_d + A_{rod} \cdot \frac{\partial P}{\partial x_d} \right) \cdot \frac{1}{M_d} \tag{34}$$

$$a_{23} = -\left(A_{rod} \cdot \frac{\partial P}{\partial x_p} \right) \cdot \frac{1}{M_d} \tag{35}$$

$$a_{41} = -\left(A_p \cdot \frac{\partial P}{\partial x_d} \right) \cdot \frac{1}{M_p} \tag{36}$$

$$a_{43} = -\left(K_p + A_p \cdot \frac{\partial P}{\partial x_p} \right) \cdot \frac{1}{M_p} \tag{37}$$

The only other coefficients to be calculated are those responsible for the displacer damping. Their values depend on the pressure drop between the expansion and compression spaces. The pressure drop was modeled as a sinusoidal pressure expressed as a linear combination of the piston velocity and the displacer velocity. Values for these pressure drop factors were determined by performing an SDM model simulation through a temperature range and fitting the model's recorded output to a linear curve with hot-end temperature as a parameter.

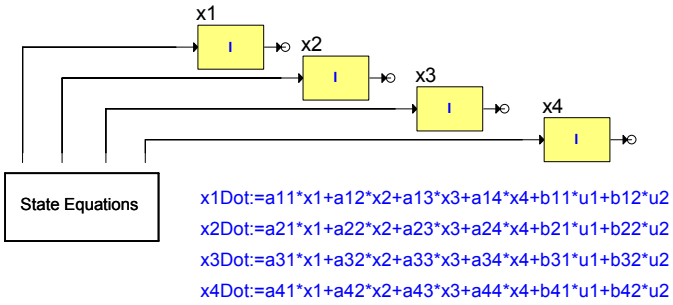

Figure 5.—Simplorer implementation of 4-state, 2-input state equation uses equation block and four integrators.

$$\frac{\partial \Delta P}{\partial \dot{x}_d} = \alpha_1 \cdot T_h + \beta_1 \tag{38}$$

$$\frac{\partial \Delta P}{\partial \dot{x}_p} = \alpha_2 \cdot T_h + \beta_2 \tag{39}$$

Finally, a_{22} and a_{24} were calculated:

$$a_{22} = A_d \cdot \frac{\partial \Delta P}{\partial \dot{x}_d} \cdot \frac{1}{M_d} \tag{40}$$

$$a_{24} = A_d \cdot \frac{\partial \Delta P}{\partial \dot{x}_p} \cdot \frac{1}{M_d} \tag{41}$$

D. Implementation

The linear models and their coupling equations were implemented in Simplorer and in Matlab/Simulink. These two high-level modeling platforms both offer convenient means to compute the integral of the state equations and to evaluate the output power and the expansion space PV power. In Simplorer, the integration of a state equation is accomplished with the block diagram of figure 5. Simulink offers a ready-made block for state equations which requires only the specification of a 4 x 4 system matrix (A-matrix) and a 4 x 2 input matrix (B-matrix) to implement the same system shown in figure 5. Implementation of the linear model also required the equations for re-computing the six A-matrix entries, and evaluating the expansion space PV power.

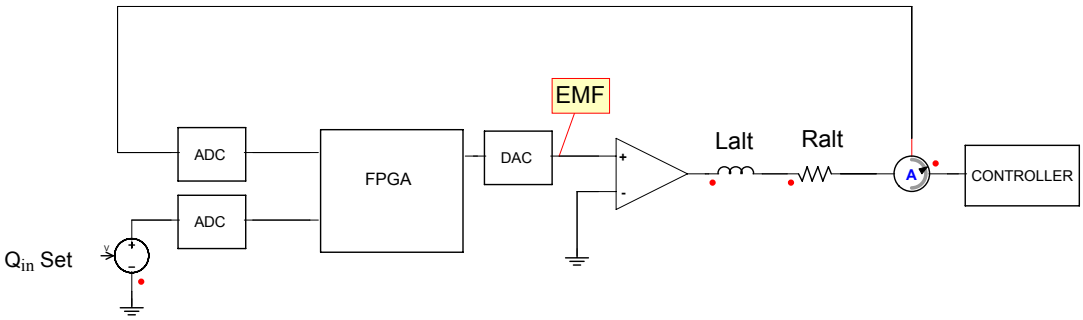

Figure 6.—Notional convertor simulator is based on the linear model running in the FPGA and producing an EMF signal in real time.

There are a number of software tools available for translating Matlab/Simulink models into code that can be executed on a microprocessor or a field-programmable gate array[6] (FPGA). The advantage of running the model on such hardware rather than on a desktop computer is that the model can simulate convertor performance in real time. With real-time simulation, the actual thermal time constants can be used in the model and more realistic response obtained. Simplorer offers a feature whereby the model shown in figure 4 can be translated into VHDL code. The feature can be used to generate a first cut of the VHDL code used to program the FPGA to execute the linear model. The code generated is not directly synthesizable—the user must first substitute the non-synthesizable variable declarations with appropriate fixed-point declarations.

By implementing the linear model on a readily-available demo board for a microprocessor or FPGA, and connecting the EMF output to a power amplifier, a convertor simulator such as that shown in figure 6 can be constructed.

The State variable representing the piston velocity is multiplied by the alternator constant and the result is used as the main output of the model. That output is equal to the alternator EMF. It is amplified in the power amplifier and the output is wired in series with an inductance and a resistance. The values used are equal to the inductance and resistance of the alternator winding. The power measured by the watt meter is the actual power output of the modeled convertor. In the case of the CTPC, it is 12.5 kW, so the amplifier in the notional schematic of figure 6 is not one that is readily available. The voltage on the load end of R_{alt} is the same as the voltage at the terminals of the convertor. Controller hardware and software can be connected and exercised. Various parameters can be changed in such a system, perhaps even while the system is running. The changes can be introduced during a controller test to verify that the controller performs as expected when the convertors endure radiator temperature changes as well as the expected radioisotope decay. The real-time simulator based on the linear model could also find use as a system for demonstrating design margins in convertor matching for dual-opposed pairs. For example, two simulators and two controllers could be used to compare system performance with spring rates matched to within 0.1, 1, and 10%.

III. Summary

The linear model described extends the four-state electro-mechanical linear model previously developed from outputs of SDM. The extended model includes a user-specified heat input and a hot-end temperature that varies with operating conditions.

Seven mathematical constructs were required in order to implement the model

1. A four-state, single-input, single-output state space model of the piston and displacer motion and damping as shown in eqs. (1) through (4).
2. A single-state, four-input, single-output state space model of the thermal processes in the hot end as shown in eqs. (12) and (13).
3. Recalculation of the mass of the working fluid in the working spaces as shown in eq. (33) whenever a change in temperature is detected.
4. Recalculation of the pressure factor of eq. (20) and associated A-matrix entries, a_{23} (eq. (33)) and a_{43} (eq. (35)) whenever a change in either temperature, amplitude or phase angle is detected.
5. Recalculation of the pressure factor of eq. (21) and associated A-matrix entries, a_{21} (eq. (32)) and a_{41} (eq. (34)) whenever a change in either temperature, amplitude or phase angle is detected.
6. Recalculation of the pressure drop factor for displacer damping with respect to displacer velocity from eq. (36) and the associated A-matrix entry a_{22} from eq. (38).
7. Recalculation of the pressure drop factor for displacer damping with respect to piston velocity from eq. (37) and the associated A-matrix entry a_{24} from eq. (39).

A possible use of the model is in Stirling convertor simulators. The simulator will generate realistic convertor electrical terminal voltages and currents so that convertor systems including controllers can be exercised under a variety of conditions.

References

1. T.F. Regan and E.J. Lewandowski, "Stirling System Modeling for Linear Dynamics Analysis," *Proceedings of the Third International Energy Conversion Engineering Conference (IECEC 2005),* San Francisco, CA, 2005.
2. M. Dhar, "Stirling Space Engine Program, Volume 1—Final Report," NASA/CR—1999-209164/VOL1.
3. M. Dhar, "Stirling Space Engine Program, Volume 2—Appendixes A, B, C, and D," NASA/CR—1999-209164/VOL2.
4. I. Urieli, and D.M. Berchowitz, *Stirling Cycle Engine Analysis*, p. 21, Adam Hilger Ltd., Bristol, 1984.
5. S. Qiu and A. Peterson , "Linear Dynamic Modeling and Numerical Simulation of an STC Stirling Convertor," *Proceedings of the 1st International Energy Conversion Engineering Conference (IECEC)*, Portsmouth, VA, 2003.
6. D. Pellerin, S. Thibault, *Practical FPGA Programming in C*, Prentice Hall, Upper Saddle River, NJ, 2005.

REPORT DOCUMENTATION PAGE	Form Approved OMB No. 0704-0188

1. REPORT DATE *(DD-MM-YYYY)*	2. REPORT TYPE	3. DATES COVERED *(From - To)*
01-12-2007	Final Contractor Report	

4. TITLE AND SUBTITLE
Development of a Linear Stirling System Model With Varying Heat Inputs

5a. CONTRACT NUMBER
NNC07TA38T

5b. GRANT NUMBER

5c. PROGRAM ELEMENT NUMBER

6. AUTHOR(S)
Regan, Timothy, F.; Lewandowski, Edward, J.

5d. PROJECT NUMBER

5e. TASK NUMBER

5f. WORK UNIT NUMBER
WBS 138494.04.01.01

7. PERFORMING ORGANIZATION NAME(S) AND ADDRESS(ES)
Sest, Inc.
18000 Jefferson Parkway
Middleburg Heights, Ohio 44130

8. PERFORMING ORGANIZATION REPORT NUMBER
E-16188

9. SPONSORING/MONITORING AGENCY NAME(S) AND ADDRESS(ES)
National Aeronautics and Space Administration
Washington, DC 20546-0001

10. SPONSORING/MONITORS ACRONYM(S)
NASA

11. SPONSORING/MONITORING REPORT NUMBER
NASA/CR-2007-215012

12. DISTRIBUTION/AVAILABILITY STATEMENT
Unclassified-Unlimited
Subject Categories: 20 and 44
Available electronically at http://gltrs.grc.nasa.gov
This publication is available from the NASA Center for AeroSpace Information, 301-621-0390

13. SUPPLEMENTARY NOTES

14. ABSTRACT
The linear model of the Stirling system developed by NASA Glenn Research Center (GRC) has been extended to include a user-specified heat input. Previously developed linear models were limited to the Stirling convertor and electrical load. They represented the thermodynamic cycle with pressure factors that remained constant. The numerical values of the pressure factors were generated by linearizing GRC's nonlinear System Dynamic Model (SDM) of the convertor at a chosen operating point. The pressure factors were fixed for that operating point, thus, the model lost accuracy if a transition to a different operating point were simulated. Although the previous linear model was used in developing controllers that manipulated current, voltage, and piston position, it could not be used in the development of control algorithms that regulated hot-end temperature. This basic model was extended to include the thermal dynamics associated with a hot-end temperature that varies over time in response to external changes as well as to changes in the Stirling cycle. The linear model described herein includes not only dynamics of the piston, displacer, gas, and electrical circuit, but also the transient effects of the heater head thermal inertia. The linear version algebraically couples two separate linear dynamic models, one model of the Stirling convertor and one model of the thermal system, through the pressure factors. The thermal system model includes heat flow of heat transfer fluid, insulation loss, and temperature drops from the heat source to the Stirling convertor expansion space. The linear model was compared to a nonlinear model, and performance was very similar. The resulting linear model can be implemented in a variety of computing environments, and is suitable for analysis with classical and state space controls analysis techniques.

15. SUBJECT TERMS
Stirling engines; Design analysis; Block diagrams; Electromechanics; Dynamics models; Simulation; AC generators; Stirling cycle; FPGA; Simulink; VHDL

16. SECURITY CLASSIFICATION OF:			17. LIMITATION OF ABSTRACT	18. NUMBER OF PAGES	19a. NAME OF RESPONSIBLE PERSON
a. REPORT	b. ABSTRACT	c. THIS PAGE			STI Help Desk (email:help@sti.nasa.gov)
U	U	U	UU	11	19b. TELEPHONE NUMBER *(include area code)* 301-621-0390